The packing of two species of polygons on the square lattice

2004 J. Phys. A: Math. Gen. 37 3085

(http://iopscience.iop.org/0305-4470/37/9/002)

INSTITUTE OF PHYSICS PUBLISHING JOURNAL OF PHYSICS A: MATHEMATICAL AND GENERAL

J. Phys. A: Math. Gen. **37** (2004) 3085–3100 PII: S0305-4470(04)71822-3

The packing of two species of polygons on the square lattice

David Dei Cont and Bernard Nienhuis

Instituut voor Theoretische Fysica, Universiteit van Amsterdam, Valckenierstraat 65, 1018 XE Amsterdam, The Netherlands

E-mail: deicont@science.uva.nl and nienhuis@science.uva.nl

Received 11 November 2003
Published 18 February 2004
Online at stacks.iop.org/JPhysA/37/3085 (DOI: 10.1088/0305-4470/37/9/002)

Abstract

We decorate the square lattice with two species of polygons under the constraint that every lattice edge is covered by only one polygon and every vertex is visited by both types of polygons. We end up with a 24-vertex model which is known in the literature as the fully packed double loop model (FPL^2). In the particular case in which the fugacities of the polygons are the same, the model admits an exact solution. The solution is obtained using coordinate Bethe ansatz and provides a closed expression for the free energy. In particular, we find the free energy of the four-colouring model and the double Hamiltonian walk and recover the known entropy of the Ice model. When both fugacities are set equal to 2 the model undergoes an infinite-order phase transition.

PACS numbers: 02.30.Ik, 05.50.+q

1. Introduction

Loop models appear in a variety of contexts: as diagrammatic expansion of the Potts and the O(n) models [30], and as models to describe polymers in several phases. The conformal properties were investigated using the Coulomb gas mapping [11]. An exact expression for the free energy, in the thermodynamic limit, was found by using the coordinate Bethe ansatz method and solving linear integral equations [16, 17]. Since then, new loop models have been studied on the square lattice [1, 22], decorated lattices [5, 34], a random lattice [15] and in three dimensions [35]. The resolution techniques have been improved both on the numerical side, introducing the connectivity basis [1, 25, 26] and on the analytical front adding the seam [19, 20], making use of the algebraic Bethe ansatz [27], mapping to an interface model [1, 7] and exploiting conformal field theory [31]. Some early examples of integrable loop models are found in [38, 39].

Here we are interested in the fully packed double loop model (FPL^2) on the square lattice. It is defined by filling the square lattice with loops in two colours, drawn along the lattice

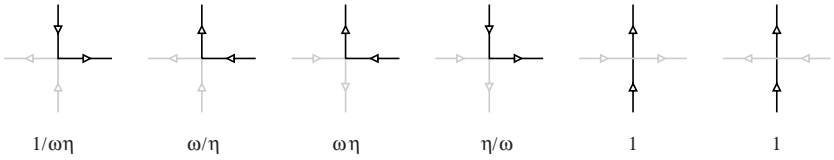

Figure 1. The six basic types of vertices of the 24-vertex model and the corresponding weights. When $\omega = \eta$ the model admits an exact solution.

edges in such a way that every bond is covered by one loop and every site is visited by both types of loops. It was introduced for the first time in [6] as an alternative representation of the four-colouring model on the square lattice. It is a natural generalization of the fully packed one loop model on the honeycomb lattice [8, 21, 24, 27], which is the loop representation of the three-colouring model on the hexagonal lattice [14].

Jacobsen and Kondev mapped the FPL^2 model onto a height model and postulate that the long wavelength behaviour is correctly described by a Liouville field theory [10]. This provides a geometrical view of conformal invariance in two-dimensional critical phenomena and a method to access the critical properties of loop models exactly. In particular, they succeed in calculating the central charge and the critical exponents [1, 9].

The FPL^2 model exhibits a rich phase diagram and provides a representation for previously studied models: Ice model [13], four-colouring model [6], dimer loop model [32], double Hamiltonian walk [10] and compact polymers [23]. A generalization of the FPL^2 model, which offers a unifying picture of the compact, dense and dilute phases of polymers, was proposed in [4] by relaxing the full packing constraint. Another possible generalization corresponds to the Flory model of polymer melting [3]. Recently the FPL^2 model has been coupled to two-dimensional quantum gravity in order to study meanders [33].

Here we find an exact expression for the free energy, in the thermodynamic limit, when the loop fugacities are the same. The solution relies on coordinate Bethe ansatz. Unfortunately the compact polymer does not belong to the solvable line. The configurational entropy for the double Hamiltonian walk [1, 10] and the four-colouring model [6] is calculated. We also confirm a conjecture on the average length of loops [2].

The present work is organized as follows. In section 2 we map the FPL^2 model into a 24-vertex model on the square lattice. The transfer matrix is set up in section 3 and diagonalized by means of coordinate Bethe ansatz (BA) in section 4. The free energy, in the thermodynamic limit, is calculated in section 5.

2. The model

We study a 24-vertex model on the square lattice. Every edge is decorated with either of two types of arrows, black or grey ones. The admitted configurations of arrows do not contain sources and sinks, so that for both colours there is one arrow going in and one going out of each vertex. The 24 possible vertices may be divided into six basic types depicted in figure 1, the others being related by $\pi/2$ rotations. We can interpret each vertex as a couple of lines turning clockwise or anticlockwise. In this way the vertex model is mapped into an oriented loop model. We are interested in the partition function of the unoriented loop model defined as,

$$Z = \sum n_b^{N_b} n_g^{N_g} \tag{1}$$

where N_b and N_g are the respective numbers of black and grey loops. We assign the fugacity n_b for black loops and n_g for grey loops. The sum is over all the allowed loop configurations. The fugacities of the loops are related to the weights of the vertex model by

$$\omega \equiv \exp(\mathrm{i}\pi e_b/4) \qquad \eta \equiv \exp(\mathrm{i}\pi e_g/4) \qquad n_b = 2\cos\pi e_b \qquad n_g = 2\cos\pi e_g. \tag{2}$$

This is the two-flavour fully packed loop model (FPL^2) on the square lattice investigated by Jacobsen and Kondev [1]. We will see that when the vertex weights are the same $\omega = \eta$, the partition function of FPL^2 (1) can be computed exactly, in the thermodynamic limit, making a coordinate Bethe ansatz. For particular values of the fugacity we recover the partition function of models studied previously. In particular $(n_b, n_g) = (2, 2)$ corresponds to the four-colouring model on the square lattice [6]. For $(n_b, n_g) = (1, 1)$ we get the Ice model solved by Lieb [13]. The single Hamiltonian walk is obtained for $(n_b, n_g) = (0, 1)$ [1]. Finally $(n_b, n_g) = (0, 0)$ is the double Hamiltonian walk for which the entropy has been correctly conjectured in [1], as we will show.

3. The transfer matrix

Here we set up a transfer matrix for the model following [13, 14]. Consider a square lattice on a cylinder, made up by LM vertices and connect the vertices by vertical and horizontal bonds. Starting from the bottom we have a circular row of L vertical bonds followed by a row of L horizontal bonds and so on alternately. Denote by $|\Psi\rangle$ the possible configuration of a row of L vertical bonds, that is to say a precise assignment of arrows on each of the vertical bonds. There are 4^L possible choices. Let $|\Psi\rangle$ and $|\Psi'\rangle$ be the states of two consecutive rows of vertical bonds. The intervening row of horizontal edges is decorated so that the L resulting vertices are of the types shown in figure 1. To each allowed configuration of vertices we assign a weight given by the product of the weight of each single vertex. Then we sum over all the possible configurations of horizontal bonds compatible with the vertical bonds and obtain the total weight denoted by $\langle\Psi'|\mathbf{T}|\Psi\rangle$. In this way we build up the transfer matrix $\mathbf{T}$ for the model. The physics of the model is encoded in the eigenvalues and the eigenvectors of the transfer matrix. If periodic boundary conditions are imposed in the vertical direction, the partition function is simply the trace of the transfer matrix raised to the power M:

$$Z = \mathrm{Tr}\,\mathbf{T}^M. \tag{3}$$

In the thermodynamic limit the free energy f_∞ follows from the largest eigenvalue $\Lambda(L)$ of the 4^L-square matrix $\mathbf{T}$ by

$$f_\infty = \lim_{L\to\infty} \frac{1}{L} \log \Lambda(L). \tag{4}$$

If we interpret the vertical axis of the cylinder as time (running downward, for convenience) and the horizontal extent as space we end up with the time evolution of a one-dimensional system.

In the following we are going to study the possible evolution of a generic state. Impose periodic boundary conditions on the horizontal direction. It is convenient to start from the state which consists of only grey arrows pointing up (pseudo-vacuum). This can match only with a successive row of grey arrows up. There are two possibilities for the intervening row of horizontal bonds: they must be black arrows, either running all to the right or all to the left. The total weight is 2. The next step is to replace some of the grey arrows up by black arrows pointing up. We call a black arrow up an *ordinary particle*. In this case the upper row can evolve in two different lower rows as illustrated by figure 2: all the particles move either one step to the right (figure 2(a)) or one step to the left (figure 2(b)). The product of the

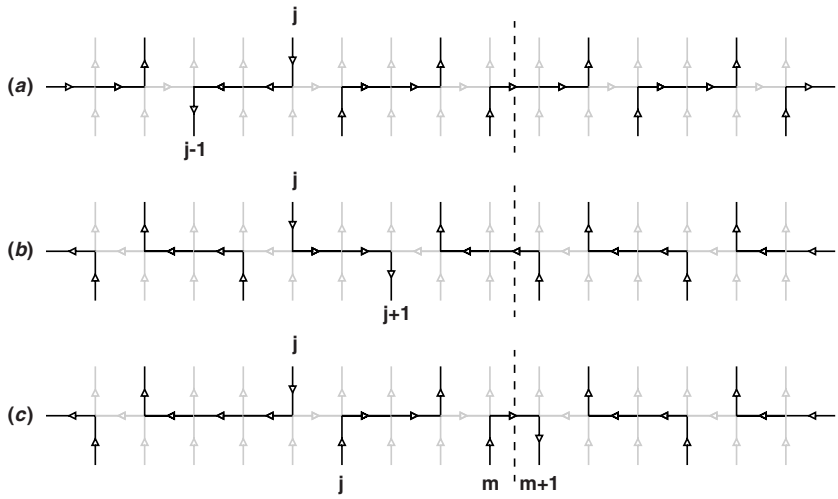

Figure 2. Four ordinary particles (black arrows up) and one special particle (black arrow down). Dashed line indicates the position of the seam. The special particle, in the upper row, is the second one from the left ($j = 2$). The possible evolutions of the upper row are: (a) shift to the right, (b) shift to the left, (c) appearance of the black half-loops. In the lower row the special particle is the fourth one ($m + 1 = 4$).

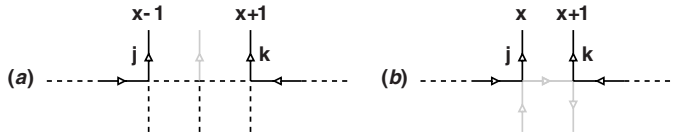

Figure 3. (a) The two particles are at a distance of two, no black loop can be inserted in between, (b) Particles on adjacent sites force a grey half-loop to be inserted.

weight of each single vertex equals 1, because vertices with reciprocal weight come in pairs, so that the total weight of the transition is set to 1. More complex patterns arise allowing for black arrows pointing down. We refer to a black arrow down as a *special particle*. Now, besides the global shift, there are other possible evolutions of which an example is depicted in figure 2(c). The special particle can be connected via a half-loop to the left or right neighbouring ordinary particle. Then in order to fulfil the boundary constraint a black half-loop has to be inserted in the lower row. This half-loop can turn either clockwise or anticlockwise and must be located between any two particles other than the two already connected via the upper row. Thus we end up with one half-loop in the upper row and one half-loop in the lower row. Particles shift one step to the right or to the left according to their position relative to the half-loops. The total weight is completely determined by the orientation of the two half-loops. A clockwise half-loop contributes ω^2 and an anticlockwise one ω^{-2}. To complete the list of allowed configurations we have to examine the states containing grey arrows down. We will interpret the grey arrow down as a bound state between two black arrows (see figures 3(b) and 4). We leave the details to the next section.

A fundamental ingredient, in seeking for an exact solution, is the existence of conserved quantities. Besides the conservation of black and grey flux, there is an additional conservation law, which is less evident. We saw that at every application of the transfer matrix, both ordinary and special particles, shift one step. Therefore the lattice can be divided into two

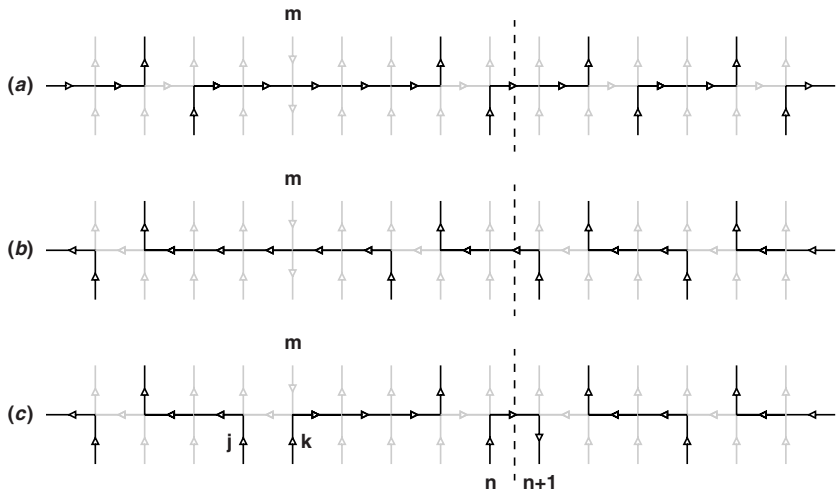

Figure 4. Four ordinary particles (black arrows up) and one bound state (grey arrow down). The bound state is the second particle from the left ($m = 2$). The possible evolutions of the upper row are: (a) the bound state goes straight and the ordinary particles shift to the right, (b) the bound state goes straight and the ordinary particles shift to the left, (c) the bound state forms a small grey half-loop and evolves splitting into two black arrows (the jth and kth particles). Periodic boundary conditions force a black-half loop to be inserted in the lower row.

sublattices such that the number of particles on each sublattice remains constant from row to row. As a result the transfer matrix splits in a series of diagonal blocks relating states in the same sector. Each sector is completely fixed by specifying the number of odd, even and special particles. We are going to diagonalize this matrix making an appropriate ansatz on the structure of the eigenvectors.

Before concluding this section we make some remarks concerning the relation between the loop and the 24-vertex model [18]. We assign the weights $\exp(\pm \mathrm{i}\pi e_{b,g})$ to each oriented loop. The orientation fixes the sign and the colour selects the phase e_b or e_g . The partition sum of the oriented FPL^2 model may be cast in the form

$$Z = \sum [\exp(\mathrm{i}\pi e_b) + \exp(-\mathrm{i}\pi e_b)]^{N_b} [\exp(\mathrm{i}\pi e_g) + \exp(-\mathrm{i}\pi e_g)]^{N_g} \tag{5}$$

where the sum runs over all the allowed unoriented loop configurations. Relating the unoriented loop fugacities to the oriented loop phases by $n_{b,g} = 2\cos \pi e_{b,g}$, we recover the partition function of the unoriented loop model (1). The advantage of splitting the loop fugacity among the two possible orientations, is that in this way the loop fugacity can be distributed along all the vertices visited by the loop. This is achieved by assigning the weight $\exp(\pm \mathrm{i}\pi e_{b,g}/4)$ to every vertex visited by the oriented loop, with + sign for a clockwise turn and $-$ for the anticlockwise one. Since for every oriented loop, on the square lattice, the difference between clockwise and anticlockwise turns is ± 4, multiplying over all the local vertex weights we recover the correct global loop weight. This should clarify relations (2) and the choices made for the vertex weights in figure 1. It is important to note that the previous argument does not work for a loop winding round the cylinder because in that case the difference between clockwise and anticlockwise turns is zero. In order to give the correct weight to non-contractable loops a seam [19–21] is placed between two generic vertices. This is well depicted in figure 2. The total weight of a generic transition will factorize in the weight of each single vertex and an extra factor which accounts for the seam. The additional factor

is set equal to a (a^{-1}) when the seam cuts a right (left) pointing arrow. For convenience we introduce a phase α setting $a = \exp(\mathrm{i}\pi\alpha)$. In terms of the phases the partition function of the unoriented FPL^2 model on the cylinder reads

$$Z = \sum (2\cos\pi e_b)^{N_b} (2\cos\pi e_g)^{N_g} (2\cos\pi\alpha)^{N_a} \tag{6}$$

where N_a is the total (black+grey) number of uncontractable loops. Note that, in order to simplify the calculation, we do not distinguish between grey and black uncontractable loops.

4. The Bethe ansatz

Since the grey arrow down serves as bound state between two black arrows, we restrict, for the moment, to the sector containing only ordinary and special particles. Denote the generic state of a row of L vertical bonds by $|\mathbf{x}, \mathbf{r}\rangle$. The vector $\mathbf{x} = (x_1, \ldots, x_N)$ gives the position of all the N particles while the vector $\mathbf{r} = (r_1, \ldots, r_m)$ specifies that those at position $x_{r_1}, \ldots, x_{r_m}$ are special ones. The eigenvalue equation for the transfer matrix reads:

$$\mathbf{T} \sum_{|\mathbf{x},\mathbf{r}\rangle} \Psi(\mathbf{x}, \mathbf{r}) |\mathbf{x}, \mathbf{r}\rangle = \Lambda \sum_{|\mathbf{x},\mathbf{r}\rangle} \Psi(\mathbf{x}, \mathbf{r}) |\mathbf{x}, \mathbf{r}\rangle \tag{7}$$

where the eigenstate of eigenvalue Λ is a linear combination, with coefficients $\Psi(\mathbf{x}, \mathbf{r})$, of the base $|\mathbf{x}, \mathbf{r}\rangle$. In the coefficients the eigenvalue equation assumes the form

$$\sum_{|\mathbf{x}',\mathbf{r}'\rangle} \langle \mathbf{x}, \mathbf{r}|\mathbf{T}|\mathbf{x}', \mathbf{r}'\rangle \Psi(\mathbf{x}', \mathbf{r}') = \Lambda \Psi(\mathbf{x}, \mathbf{r}). \tag{8}$$

Here we examine the sector with N particles in total, ($N - 1$ ordinary + 1 special), located at position $x_1, \ldots, x_N$, where $x_{i+1} - x_i > 2$, and suppose that the jth particle is a special one. Moreover, we assume that the seam is placed between two ordinary particles. In order to solve the eigenvalue problem we make the following ansatz on the form of the wavefunction:

$$\Psi_j(x_1, \ldots, x_N) \equiv \sum_{\mathbf{p}} A_{p_1 \ldots p_N} \psi_j(\mathbf{p}) \prod_{i=1}^{N} z_{p_i}^{x_i} \tag{9}$$

where the sum runs over all permutations $\mathbf{p} = (p_1, \ldots, p_N)$ of the numbers $1, \ldots, N$. The goal is to choose $A_{\mathbf{p}}$, $\psi_j(\mathbf{p})$ and the complex numbers $z_{p_1}, \ldots, z_{p_N}$ so that (8) is satisfied. At this stage the structure of the coefficient $\psi_j(\mathbf{p})$, the behaviour of $A_{p_1 \ldots p_N}$ under the exchange of two consecutive indices, and the dependence of the eigenvalue Λ on $z_{p_1}, \ldots, z_{p_N}$, are still unknown. In the following we are going to determine it.

Inserting ansatz (9) into the eigenvalue equation (8), we see that a sufficient condition for the validity of (8) is that the coefficient $\psi_j(\mathbf{p})$ obeys, for any permutation $\mathbf{p}$, the following evolution equation:

$$\begin{aligned}\Lambda \psi_j = {} & a z_{1:N} \psi_{j-1} + \frac{1}{a z_{1:N}} \psi_{j+1} + \omega^2 \sum_{m=j}^{j+N-2} (\omega^{-2} \alpha_m \psi_m + \omega^2 \beta_{m+1} \psi_{m+1}) \frac{z_{j:m}}{z_{m+1:N+j-1}} \\ & + \omega^{-2} \sum_{m=j+1}^{j+N-1} (\omega^{-2} \alpha_m \psi_m + \omega^2 \beta_{m+1} \psi_{m+1}) \frac{z_{j+1:m}}{z_{m+1:N+j}}.\end{aligned} \tag{10}$$

Since we will be concerned mainly with one permutation $\mathbf{p}$, we introduce the more compact notation $z_i \equiv z_{p_i}$ and $z_{i:k} \equiv \prod_{j=i}^{k} z_{p_j}$, together with the cyclic condition $z_j = z_{j+N}$. Let us examine in detail all the terms. The first term on the rhs of (10) describes the process in which all the particles shift one step to the right (figure 2(a)). Note that the special particle is the

jth one in the upper row and the $(j-1)$th in the lower row. The weight of the process is a because the arrow crosses the seam in the right direction. The product $z_{1:N}$ accounts for the global shift to the right. The second term describes the left translation (figure 2(b)). Let us clarify the two sums. Start with the first one (figure 2(c)). The special particle in the upper row is connected via a clockwise half-loop to the left neighbouring ordinary particle. This is taken into account by the coefficient ω^2 in front of the sum. The half-loop in the lower row must be inserted between any two particles except the ones already connected by a half-loop in the upper row. Therefore the sum runs from $m = j$ to $m = j + N - 2$. Moreover the particles distributed between the jth and mth particles undergo a shift to the right while those positioned between $m + 1$ and $j + N - 1$ move one step to the left. These translations are taken into account by the products $z_{j:m}/z_{m+1:N+j-1}$. Since the half-loop in the lower row may turn clockwise or anticlockwise, each term in the sum splits in two parts: $\omega^{-2}\psi_m$ for the anticlockwise half-loop and $\omega^2\psi_{m+1}$ for the clockwise one. The same argument applies to the second sum. The coefficients α_m and β_{m+1} ensure that loops which wrap around the cylinder pick up the correct weight. They are set equal to a (a^{-1}) when an arrow, of any of the two colours, in the intervening row of horizontal edges, crosses the seam in the right (left) direction. Their values depend on the relative position of the special particle in the upper row, the seam, and the half-loop in the lower row. Following figure 2(c) we see that when the lower half-loop is placed between the special particle j and the seam, the intervening arrow, cut by the seam, points to the left, so that $\alpha_m = \beta_{m+1} = a^{-1}$. When it is positioned on the right of the seam $\alpha_m = \beta_{m+1} = a$. In the special case in which the seam cuts the lower half-loop $\alpha_m = a^{-1}$ and $\beta_{m+1} = a$.

Our aim is to compute the coefficient ψ_j and the eigenvalue Λ. Rearranging the terms, equation (10) may be expressed in a more compact form as

$$\Lambda\psi_j = -az_{1:N}\omega^4\psi_j - \frac{1}{az_{1:N}\omega^4}\psi_j + \left(z_j^{-1}\omega^{-2} + z_j\omega^2\right)Q_j \tag{11}$$

where the quantity Q_j is defined as

$$Q_j \equiv \sum_{m=j}^{j+N-1} (\omega^{-2}\alpha_m\psi_m + \omega^2\beta_{m+1}\psi_{m+1})\frac{z_{j+1:m}}{z_{m+1:N+j-1}}. \tag{12}$$

The term Q_j generates all the oriented black half-loops in the lower row, which can be accommodated between two consecutive particles. An alternative definition of Q_j comes from equation (11):

$$Q_j = \frac{\Lambda + az_{1:N}\omega^4 + a^{-1}z_{1:N}^{-1}\omega^{-4}}{z_j^{-1}\omega^{-2} + z_j\omega^2}\psi_j. \tag{13}$$

From the original definition of Q_j (12) it follows that

$$z_{j+1}Q_{j+1} - z_j^{-1}Q_j = (\omega^{-2}\psi_j + \omega^2\psi_{j+1})\left(az_{1:N} - \frac{1}{az_{1:N}}\right). \tag{14}$$

Substituting in the lhs of (14) the alternative expression for Q_j given by (13):

$$\begin{aligned}\left(\Lambda + az_{1:N}\omega^4 + a^{-1}z_{1:N}^{-1}\omega^{-4}\right)&\left(\frac{z_{j+1}^2}{\omega^{-2} + z_{j+1}^2\omega^2}\psi_{j+1} - \frac{1}{\omega^{-2} + z_j^2\omega^2}\psi_j\right)\\ &= (\omega^{-2}\psi_j + \omega^2\psi_{j+1})\left(az_{1:N} - \frac{1}{az_{1:N}}\right).\end{aligned} \tag{15}$$

Equation (15) can be read as a recursive relation for ψ_j. It simplifies defining the eigenvalue via a new variable μ:

$$\Lambda \equiv -\left[az_{1:N}(\omega^4 - \mu) + \frac{1}{az_{1:N}}(\omega^{-4} + \mu) \right]. \tag{16}$$

Replacing the eigenvalue Λ in equation (15) by definition (16) and dropping the overall factor which contains $az_{1:N}$, the recursive relation for ψ_j reads

$$\frac{(\mu - \omega^4)z_{j+1}^2 - 1}{\omega^{-2} + z_{j+1}^2\omega^2}\psi_{j+1} = \frac{\mu + z_j^2 + \omega^{-4}}{\omega^{-2} + z_j^2\omega^2}\psi_j. \tag{17}$$

Note that relation (17) does not involve the parameter a. To see how the parameter a enters in the wavefunction we have to inspect the case in which there are no ordinary particles between the seam and the special particle. Note that in this special case the seam may cut the upper black half-loop. We skip the calculation and give the final result for the structure of the coefficient ψ_m:

$$\psi_m = s\frac{\omega^{-2} + \omega^2 z_m^2}{(\mu - \omega^4)z_m^2 - 1}\prod_{k=1}^{m-1}\frac{\mu + \omega^{-4} + z_k^2}{(\mu - \omega^4)z_k^2 - 1} \tag{18}$$

where $s = 1$ if the special particle is located left of the seam, and $s = a^{-2}$ if it is positioned on the right side.

The formalism developed up to now, works for sparsely distributed particles. When the condition $x_{i+1} - x_i > 2$ does not hold, several restrictions on the amplitude $A_{\mathbf{p}}$ are necessary. Suppose that two generic particles are located at positions $x - 1$ and $x + 1$ (see figure 3(*a*)), then a half-loop of black arrows cannot be inserted between them in the lower row. Thus, this event must be omitted from the generic list of possibilities, in which both the particles have come from afar. We demand the weight of the corresponding term, automatically generated by the lhs of the eigenvalue equation (8), when the particles are sparse, to be zero in this special case:

$$\sum_{j\leftrightarrow k} A_{\ldots jk\ldots}(\omega^{-2}\alpha_m\psi_m + \omega^2\beta_{m+1}\psi_{m+1})z_j^x z_k^x = 0 \tag{19}$$

where the sum is over the interchange $j \leftrightarrow k$ of the indices and the short-hand notation $A_{\ldots jk\ldots} \equiv A_{\ldots p_j p_k \ldots}$ has been used. The way in which the momenta z_j and z_k enter in the coefficients ψ_m and ψ_{m+1} can be read from the structure of (18). Inserting (18) in equation (19) and working out we see that only terms proportional to μ survive. The resulting requirement for the scattering factor is

$$\frac{A_{\ldots jk\ldots}}{A_{\ldots kj\ldots}} = -\frac{1 + (\omega^4 + \omega^{-4})z_j^2 + z_j^2 z_k^2}{1 + (\omega^4 + \omega^{-4})z_k^2 + z_j^2 z_k^2}. \tag{20}$$

Let us make the following important observation: the transfer matrix acts on a generic state shifting each particle one step to the right or to the left. Thus we can group particles in two sets according to their position: *odd* and *even* particles. The two families do not mix. This means that the scattering relation (20) holds for particles belonging to the same family.

In the following we elaborate our formalism in order to incorporate states containing grey arrows pointing down. Start by noting that black arrows positioned on adjacent sites generate a half-loop of grey arrows (see figure 3(*b*)). This observation leads to treat the grey arrow down as bound state of two generic particles. Consider the states with $N - 2$ ordinary particles

(black arrows up) and 1 bound state (grey arrow down). We make the following natural ansatz on the form of the wavefunction:

$$\Phi_m(x_1,\ldots,x_m,\ldots x_{N-1}) \equiv \sum_{\mathbf{p}} A_{p_1\ldots p_N}\phi_m(\mathbf{p})\left[z_{p_1}^{x_1}\ldots(z_{p_m}z_{p_{m+1}})^{x_m}\ldots z_{p_N}^{x_{N-1}}\right] \tag{21}$$

where the index m indicates that the bound state is preceded by $m-1$ ordinary particles. The bound state is located at position x_m. Note that the wavefunctions (21) and (9) have essentially the same structure apart from the coefficient ϕ_m which is still unknown at this stage. In order to compute it we work out the eigenvalue equation (8) with the help of the ansatz (21) and (9) for the particular case in which the initial state (rhs of equation (8)) contains two adjacent particles. We see that if we require that

$$\sum_{j\leftrightarrow k} A_{\ldots jk\ldots}(\omega^{-2}\psi_m+\omega^2\psi_{m+1})z_j = \sum_{j\leftrightarrow k} A_{\ldots jk\ldots}\phi_m(\eta^{-2}+\eta^2 z_j z_k) \tag{22}$$

then the generic list of possible evolutions (see rhs of equation (10)) automatically incorporates the grey half-loop. The coefficient η accounts for the two possible orientations of the grey half-loop. The next step is to study the evolution of the bound state. The analogue of equation (10) for the bound state reads

$$\Lambda\sum_{j\leftrightarrow k} A_{\ldots jk\ldots}\phi_m = \sum_{j\leftrightarrow k} A_{\ldots jk\ldots}\left[\phi_m\left(\frac{z_jz_k}{z_{1:N}a}+\frac{z_{1:N}a}{z_jz_k}\right)\right.$$
$$\left.+\left(\eta^{-2}z_k+\frac{\eta^2}{z_j}\right)\sum_{n=m+1}^{m+N-1}\frac{z_{m+2:n}}{z_{n+1:m+N-1}}(\omega^{-2}\alpha_n\psi_n+\omega^2\beta_{n+1}\psi_{n+1})\right]. \tag{23}$$

The bound state can move straight or form a half-loop as shown in figure 4. Now we have to check the consistency of equation (23). For that eliminate ϕ_m in equation (23) using relation (22). In order to eliminate Λ, plug in the value of $\Lambda\psi_j$ given by the rhs of the evolution equation (10). At the end we get an expression relating ψ_j for different values of j. In the appendix we will show that such expression is consistent if we choose the same value for the vertex weights $\omega=\eta$ (in terms of phases $e_b=e_g$) and demand that the scattering amplitude is symmetric for the interchange of particles belonging to *different* families:

$$A_{\ldots jk\ldots} = A_{\ldots kj\ldots}. \tag{24}$$

Note that the new scattering relation (24) is not in contradiction with the previous relation (20) since the new one involves particles of *different* families.

We went further and studied the sector with two special particles. As amplitude ψ_{jk}, for two special particles, we take a linear combination of $\psi_j(\mu_1)\psi_k(\mu_2)$ and $\psi_j(\mu_2)\psi_k(\mu_1)$. We call B_{12} and B_{21} the relative scattering amplitudes. The cancellation of unwanted terms [13] that arise in the expression for the eigenvalue determines the ratio between B_{12} and B_{21}. Anticipating on the sector with more special particles we write the scattering relation in the more general form

$$\frac{B_{\ldots ij\ldots}}{B_{\ldots ji\ldots}} = -\frac{\mu_i\mu_j+\omega^{-4}\mu_j-\omega^4\mu_i}{\mu_i\mu_j+\omega^{-4}\mu_i-\omega^4\mu_j}. \tag{25}$$

Now we have all the ingredients to derive the Bethe ansatz equations. In the spirit of coordinate nested Bethe ansatz [14] we are ready to formulate an ansatz for the state with any number of special particles:

$$\Psi(x_1,\ldots,x_N|r_1,\ldots,r_m) = \sum_{\mathbf{p},\mathbf{q}} A_{\mathbf{p}}B_{\mathbf{q}}\prod_{j=1}^{N} z_{p_j}^{x_j}\prod_{i=1}^{m}\psi_i(\mathbf{p},\mu_{q_i},r_i) \tag{26}$$

where the one special particle amplitude (18) is given by

$$\psi_i(\mathbf{p},\mu,r_i) = s\frac{\omega^{-2}+\omega^2 z_{p_{r_i}}^2}{(\mu-\omega^2)z_{p_{r_i}}^2-1}\prod_{k=1}^{r_i-1}\frac{\mu+\omega^{-4}+z_{p_k}^2}{(\mu-\omega^4)z_{p_k}^2-1}. \tag{27}$$

The wavefunction has to satisfy periodic boundary conditions. Suppose that the first particle is an ordinary one ($r_1 \neq 1$):

$$\Psi(x_1,\ldots,x_N|r_1,\ldots,r_m) = \Psi(x_2,\ldots,x_N,x_1+L|r_1-1,\ldots,r_m-1). \tag{28}$$

From ansatz (26), it follows that a sufficient condition for the validity of (28) is that the complex variable z_{p_1} fulfils, for every permutation $\mathbf{p}$, the relation

$$A_{p_1\ldots p_N}\prod_{i=1}^{m}\frac{\mu_{q_i}+\omega^{-4}+z_{p_1}^2}{(\mu_{q_i}-\omega^4)z_{p_1}^2-1} = A_{p_2\ldots p_N p_1}z_{p_1}^L. \tag{29}$$

We make the additional assumption that the system has an even length L, this means that after having imposed periodic boundary conditions to a generic particle the sublattice to which the particle belongs does not change. We associate momenta z_j ($j=1,\ldots,n_z$) with the even sublattice and y_j ($j=1,\ldots,n_y$) with the odd sublattice. By eliminating the amplitudes in (29) using relations (20) and (24), we get the first two families of BA equations:

$$\prod_{i=1}^{n_\mu}\frac{\mu_i+\omega^{-4}+z_j^2}{(\mu_i-\omega^4)z_j^2-1}\prod_{k\neq j}^{n_z}-\frac{1+(\omega^4+\omega^{-4})z_j^2+z_j^2z_k^2}{1+(\omega^4+\omega^{-4})z_k^2+z_j^2z_k^2} = z_j^L \tag{30}$$

$$\prod_{i=1}^{n_\mu}\frac{\mu_i+\omega^{-4}+y_j^2}{(\mu_i-\omega^4)y_j^2-1}\prod_{k\neq j}^{n_y}-\frac{1+(\omega^4+\omega^{-4})y_j^2+y_j^2y_k^2}{1+(\omega^4+\omega^{-4})y_k^2+y_j^2y_k^2} = y_j^L. \tag{31}$$

Similarly, assuming that the first particle is a special one, we find an equation for the variable μ_{q_1}:

$$B_{q_1\ldots q_m} = B_{q_2\ldots q_m q_1}\prod_{k=1}^{N}\frac{\mu_{q_1}+\omega^{-4}+z_{p_k}^2}{(\mu_{q_1}-\omega^4)z_{p_k}^2-1}. \tag{32}$$

Making use of relation (25) we get the third family of BA equations:

$$a^{-2}\prod_{j=1}^{n_z}\frac{\mu_l+\omega^{-4}+z_j^2}{(\mu_l-\omega^4)z_j^2-1}\prod_{k=1}^{n_y}\frac{\mu_l+\omega^{-4}+y_k^2}{(\mu_l-\omega^4)y_k^2-1}\prod_{m\neq l}^{n_\mu}-\frac{\mu_m\mu_l+\omega^{-4}\mu_l-\omega^4\mu_m}{\mu_m\mu_l+\omega^{-4}\mu_m-\omega^4\mu_l} = 1. \tag{33}$$

The factor a^{-2} arises due to the fact that the special particle moves from the left to the right side of the seam when periodic boundary conditions are imposed.

The eigenvalue expression that generalizes (16) has the form

$$\Lambda = (-1)^{n_\mu}\left[a\prod_{j=1}^{n_z}z_j\prod_{k=1}^{n_y}y_k\prod_{m=1}^{n_\mu}(\omega^4-\mu_m)+\frac{1}{a}\prod_{j=1}^{n_z}\frac{1}{z_j}\prod_{k=1}^{n_y}\frac{1}{y_k}\prod_{m=1}^{n_\mu}\left(\frac{1}{\omega^4}+\mu_m\right)\right]. \tag{34}$$

5. The free energy

In order to find an exact solution of the model in the thermodynamic limit we need difference kernels [13]. First simplify a bit notation (2) introducing the phase $\theta \equiv e_b = e_g$ and reminding that $a = \exp(\mathrm{i}\pi\alpha)$. Then introduce a new set of variables u_j, v_j, w_j related to z_j, y_j, μ_j by

$$z_j^2 = \frac{\sin\frac{\pi\theta}{2}(1+u_j\mathrm{i})}{\sin\frac{\pi\theta}{2}(1-u_j\mathrm{i})} \qquad y_j^2 = \frac{\sin\frac{\pi\theta}{2}(1+v_j\mathrm{i})}{\sin\frac{\pi\theta}{2}(1-v_j\mathrm{i})} \qquad \mu_j = \frac{2\mathrm{i}\sin\pi\theta}{1-\exp(\pi\theta w_j)} \tag{35}$$

and define the function

$$S_c(x,\theta) \equiv \frac{\sin\frac{\pi\theta}{2}(c+x\mathrm{i})}{\sin\frac{\pi\theta}{2}(c-x\mathrm{i})}. \tag{36}$$

The BAE in the new variables are

$$S_1(u_j,\theta)^{L/2} = -\prod_{i=1}^{n_w} S_1(w_i-u_j,\theta)\prod_{k=1}^{n_u} -S_2(u_j-u_k,\theta) \tag{37}$$

$$S_1(v_j,\theta)^{L/2} = -\prod_{i=1}^{n_w} S_1(w_i-v_j,\theta)\prod_{k=1}^{n_v} -S_2(v_j-v_k,\theta) \tag{38}$$

$$\exp(-2\mathrm{i}\pi\alpha)\prod_{j=1}^{n_u} S_1(w_l-u_j,\theta)\prod_{k=1}^{n_v} S_1(w_l-v_k,\theta)\prod_{m=1}^{n_w} -S_2(w_m-w_l,\theta) = -1. \tag{39}$$

The eigenvalue is the sum of two terms:

$$\Lambda = (-1)^{n_w}\left[\exp(\mathrm{i}\pi\alpha)\prod_{j=1}^{n_u} S_1(u_j,\theta)^{1/2}\prod_{k=1}^{n_v} S_1(v_k,\theta)^{1/2}\prod_{m=1}^{n_w}\frac{\sin\frac{\pi\theta}{2}(w_m\mathrm{i}-2)}{\sin\frac{\pi\theta}{2}w_m\mathrm{i}}\right.$$
$$\left. + \exp(-\mathrm{i}\pi\alpha)\prod_{j=1}^{n_u} S_1(u_j,\theta)^{-1/2}\prod_{k=1}^{n_v} S_1(v_k,\theta)^{-1/2}\prod_{m=1}^{n_w}\frac{\sin\frac{\pi\theta}{2}(w_m\mathrm{i}+2)}{\sin\frac{\pi\theta}{2}w_m\mathrm{i}}\right]. \tag{40}$$

Following the argument of [13] we see that the dominant eigenvalue lies in the sector labelled by ($n_u = n_v = n_w = L/2$). In the ground-state sector the number of black arrows up equals the number of black arrows down. Also the number of grey arrows up and down are the same. Note that the total number of black and grey arrows are allowed to fluctuate due to formation of bound states. For $\alpha = 0$ we get the largest eigenvalue when the roots are symmetrically distributed on the real axis in such a way that no holes appear between two consecutive roots (close packing of the roots). Switching on the twist α, the root distributions start to drift. The seam breaks translational invariance, but because the location of the seam is immaterial, this is not a physical effect. The pseudo-translational invariance of the ground state is expressed as

$$\prod_{j=1}^{n_u} S_1(u_j,\theta)^{1/2}\prod_{k=1}^{n_v} S_1(v_k,\theta)^{1/2} = \exp(\mathrm{i}\pi\alpha), \tag{41}$$

Which allows for an eigenvalue expression with just one term:

$$\Lambda = A\prod_{m=1}^{n_w}\left(\cos^2\pi\theta + \sin^2\pi\theta\coth^2\frac{\pi\theta w_m}{2}\right)^{1/2}. \tag{42}$$

And the α dependence has been encapsulated in the factor A:

$$A \equiv 2\cos\left(2\pi\alpha + \sum_{m=1}^{n_w}\arctan\left(\tan\pi\theta\coth\left(\frac{\pi\theta w_m}{2}\right)\right)\right). \tag{43}$$

We can go further with the simplification taking the logarithm. For that purpose define the function

$$\phi_c(x,\theta) \equiv \mathrm{i}\log S_c(x,\theta). \tag{44}$$

And introduce the counting functions $Z_L(x,\theta)$ as follows:

$$Z_{L,u}(u,\theta) \equiv -\frac{L}{2}\phi_1(u,\theta) + \sum_{m=1}^{n_w}\phi_1(w_m - u,\theta) - \sum_{k=1}^{n_u}\phi_2(u_k - u,\theta) \tag{45}$$

$$Z_{L,v}(v,\theta) \equiv -\frac{L}{2}\phi_1(v,\theta) + \sum_{m=1}^{n_w}\phi_1(w_m - v,\theta) - \sum_{k=1}^{n_v}\phi_2(v_k - v,\theta) \tag{46}$$

$$Z_{L,w}(w,\theta) \equiv \sum_{j=1}^{n_u}\phi_1(u_j - w,\theta) + \sum_{k=1}^{n_v}\phi_1(v_k - w,\theta) - \sum_{m=1}^{n_w}\phi_2(w_m - w,\theta) - 2\pi\alpha. \tag{47}$$

Note that the counting functions defined in this way have positive derivatives. The next step is to define the root density function via the derivative of the counting functions in the thermodynamic limit:

$$\rho(x) = \frac{1}{2\pi}\lim_{L\to\infty}\frac{\mathrm{d}}{\mathrm{d}x}\frac{Z_L(x)}{L}. \tag{48}$$

Numerically we find that approaching the thermodynamic limit the roots spread over the real axis, from $-\infty$ to $+\infty$, thus the integral equations for the root density functions are

$$\rho_u(u,\theta) = -\frac{1}{4\pi}\phi_1'(u,\theta) + \frac{1}{2\pi}\int_{-\infty}^{\infty}[\phi_1'(x-u,\theta)\rho_w(x,\theta) - \phi_2'(x-u,\theta)\rho_u(x,\theta)]\,\mathrm{d}x \tag{49}$$

$$\rho_v(v,\theta) = -\frac{1}{4\pi}\phi_1'(v,\theta) + \frac{1}{2\pi}\int_{-\infty}^{\infty}[\phi_1'(x-v,\theta)\rho_w(x,\theta) - \phi_2'(x-v,\theta)\rho_v(x,\theta)]\,\mathrm{d}x \tag{50}$$

$$\rho_w(w,\theta) = \frac{1}{2\pi}\int_{-\infty}^{\infty}[\phi_1'(x-w,\theta)(\rho_u(x,\theta)+\rho_v(x,\theta)) - \phi_2'(x-w,\theta)\rho_w(x,\theta)]\,\mathrm{d}x. \tag{51}$$

The system can be solved using Fourier transform. The solutions for the root density functions are

$$\rho_w(x) = \frac{1}{8}\operatorname{sech}\left(\frac{\pi x}{4}\right) \qquad \rho_u(x) = \rho_v(x) = \frac{\sqrt{2}}{8}\operatorname{ch}\left(\frac{\pi x}{4}\right)\operatorname{sech}\left(\frac{\pi x}{2}\right). \tag{52}$$

It is remarkable to note that they do not depend on the parameter θ. There is still θ dependence in the expression for the largest eigenvalue (42). The free energy in the thermodynamic limit has the following integral representation:

$$f_\infty(\theta) = \frac{1}{16}\int_{-\infty}^{\infty}\log\left[\cos^2\pi\theta + \sin^2\pi\theta\coth^2\frac{\pi\theta x}{2}\right]\operatorname{sech}\left(\frac{\pi x}{4}\right)\mathrm{d}x \qquad 0 < \theta \leqslant 1. \tag{53}$$

Note that the α dependence (43) drops out in the thermodynamic limit. In the interval $1/2 < \theta = e_b = e_g \leqslant 1$ according to relations (2) the fugacity of the loops becomes negative so that the partition sum (1) will also contain configurations with a negative weight. We checked numerically with 15 digits of accuracy that at $\theta = 1$, the largest eigenvalue of the transfer matrix is 2 so that the free energy vanishes. Applying Parseval formula we can write the free energy as a Laplace transform:

$$f_\infty(\theta) = -\int_0^\infty \frac{\mathrm{e}^{-p}\operatorname{sech}(2p\theta)\sinh^2(p\theta)}{p\sinh p}\,\mathrm{d}p - \frac{1}{2}\log 2 - \frac{3}{2}\log\pi + 2\log\Gamma(1/4). \tag{54}$$

For particular values of θ the integral can be solved [13].

Two mutually excluding Hamiltonian walks [1]:

$$f_\infty(1/2) = \tfrac{1}{2}\log 2. \tag{55}$$

The Ice model [13]

$$f_\infty(1/3) = \tfrac{3}{2}\log\tfrac{4}{3}. \tag{56}$$

Four-colouring on the square lattice [1, 6]:

$$f_\infty(\theta \to 0) = -\tfrac{1}{2}\log 2 - \tfrac{3}{2}\log\pi + 2\log\Gamma(1/4). \tag{57}$$

Note that in this last particular limit expression (36) becomes rational. These BA equations were derived for the first time in [12] and look very much like those derived in [29] for mixed SU(N) vertex model for the case $N = 4$. The BA equations for SU(N) vertex models were derived in [28] starting from a Yang–Baxter structure in which the R-matrix and the Lax operator coincide. Martins [29] using the Braid-monoid algebra constructed a more general monodromy matrix mixing two distinct Lax operators.

An exact solution can also be found in the non-critical region which corresponds to fugacity $n > 2$. Since the fugacity is defined by $n = 2\cos\pi\theta$, this region corresponds to imaginary values for the parameter θ. For convenience we assume θ real so that the fugacity is now given by $n = 2\cosh\pi\theta$, and redefine the function (36) and (44) by

$$\phi_c(x,\theta) \equiv \mathrm{i}\log\left(\frac{\sinh\frac{\pi\theta}{2}(c + x\mathrm{i})}{\sinh\frac{\pi\theta}{2}(c - x\mathrm{i})}\right). \tag{58}$$

Now in the thermodynamic limit, the roots corresponding to the largest eigenvalue are symmetrically distributed in the finite interval $[-1/\theta, 1/\theta]$. This time the integral equation can be solved by Fourier series. The Fourier components are

$$\widehat{\rho_u}(m,\theta) = \widehat{\rho_v}(m,\theta) = \tfrac{1}{2}\cosh(m\pi\theta)\,\mathrm{sech}(2m\pi\theta) \qquad \widehat{\rho_w}(m,\theta) = \tfrac{1}{2}\,\mathrm{sech}(2m\pi\theta). \tag{59}$$

The root density functions

$$\rho_w(x,\theta) = \frac{\theta}{2}\sum_{m=-\infty}^{+\infty}\widehat{\rho_w}(m,\theta)\exp(\mathrm{i}m\pi\theta x) \qquad \rho_{u,v}(x,\theta) = \frac{\theta}{2}\sum_{m=-\infty}^{+\infty}\widehat{\rho_{u,v}}(m,\theta)\exp(\mathrm{i}m\pi\theta x). \tag{60}$$

These can also be written in terms of Jacobi elliptic functions:

$$\rho_w(x,\theta) = \frac{\theta K(k)}{2\pi}\,\mathrm{dn}[xK(k)\theta, k] \tag{61}$$

$$\rho_{u,v}(x,\theta) = \frac{\theta K(k)}{4\pi}\left(\mathrm{dn}[xK(k)\theta + \mathrm{i}K(k)\theta, k] + \mathrm{dn}[xK(k)\theta - \mathrm{i}K(k)\theta, k]\right) \tag{62}$$

where the modulus k and the complete elliptic integral of the first kind $K(k)$ are related to the phase θ by

$$K(k) \equiv \int_0^{\pi/2}[1 - k^2\sin^2\phi]^{-1/2}\,\mathrm{d}\phi \qquad \frac{K(\sqrt{1-k^2})}{K(k)} = 2\theta. \tag{63}$$

The free energy

$$f_\infty(\theta) = \frac{\pi\theta}{2} + \sum_{m=1}^{\infty}\frac{\mathrm{e}^{-m\pi\theta}\sinh(m\pi\theta)}{m\cosh(2m\pi\theta)} = -\frac{1}{4}\log q + \sum_{m=1}^{\infty}\frac{1}{m}\frac{1-q^m}{q^m+q^{-m}} \tag{64}$$

where $q \equiv \exp(-2\pi\theta)$. Taylor expanding the summand around $q = 0$ and summing with respect to m we get the following product expansion for the partition function:

$$\lim_{L,M\to\infty} Z^{1/LM} = \mathrm{e}^{f_\infty(\theta)} = q^{-1/4}\prod_{p=1}^{\infty}\frac{(1-q^{2(2p-1)})(1-q^{4p-1})}{(1-q^{4p-3})(1-q^{4p})}. \tag{65}$$

For $q \to 1$ we get the partition function for the four-colouring model:

$$e^{f_\infty(0)} = \prod_{p=1}^{\infty} \frac{(2p-1)(4p-1)}{2p(4p-3)} = \frac{\Gamma^2(1/4)}{\sqrt{2}\pi^{3/2}} \tag{66}$$

in agreement with the expression (57).

We have all the ingredients to discuss the singular behaviour of the free energy. We can read the non-analyticity of the partition function from expression (65). It appears that (65) has a solid wall of singularities on the unit circle [14]. Following [36, 37] we calculate the analytic continuation of the critical free energy (54) into the non-critical region so that we can extract the singularity of the free energy near the critical point $n = 2$. We find that near $n = 2$ the free energy has an essential singularity:

$$f_{\text{sing}} \propto \exp\left(-\frac{\pi^2}{4|n-2|^{1/2}}\right). \tag{67}$$

This means that at the critical point $n = 2$ the model undergoes an infinite-order phase transition of the Kosterlitz–Thouless type. The same type of transition has been found in [27] for a loop model on the hexagonal lattice. Even if the free energy exhibits an essential singularity at $n = 2$, the right and left derivatives, of generic order, approach the same values, in the limit $n \to 2^{\pm}$.

For the first derivative we get

$$\left.\frac{\mathrm{d}f_\infty(n)}{\mathrm{d}n}\right|_{n\to 2^{\pm}} = \frac{1}{24}. \tag{68}$$

It has been shown that the first-order derivative of the free energy with respect to the fugacity is related to the average loop length $\overline{L}$ [2]. We found $\overline{L} = 12$, which is three times the minimal loop length allowed by the square lattice, in agreement with the conjecture made in [2].

6. Conclusions

We have studied the bulk properties of the FPL^2 model in the case in which the two loop fugacities are the same, both in the critical ($n \leqslant 2$) and non-critical ($n > 2$) regions. The model undergoes an infinite-order phase transition, of the Kosterlitz–Thouless type, at the critical point $n = 2$. The ansatz we make on the wavefunction works only when the vertex weights are the same $\omega = \eta$. This is because the amplitude that describes the scattering of particles belonging to different (odd and even) families, does not factorize into two particles scattering amplitudes when $\omega \neq \eta$. The details are in the appendix. It will be interesting to find the Yang–Baxter relation on this solvable line and hopefully extend it to the whole phase diagram. Using the nonlinear integral equation method we found the exact value of the central charge and of some scaling dimensions, on the solvable line. We will publish the results in a forthcoming paper.

Appendix

Replacing ϕ_m in equation (23) by equation (22) the consistency requirement becomes

$$\sum_{j\leftrightarrow k} A_{\ldots jk\ldots}\left[\left(\frac{z_j z_k}{z_{1:N}a} + \frac{z_{1:N}a}{z_j z_k} - \Lambda\right)(\omega^{-2}\psi_m + \omega^2\psi_{m+1})z_j + (\eta^{-2} + \eta^2 z_j z_k)\right.$$
$$\left.\times\left(\eta^{-2}z_k + \frac{\eta^2}{z_j}\right)\sum_{n=m+1}^{m+N-1}\frac{z_{m+2:n}}{z_{n+1:m+N-1}}(\omega^{-2}\alpha_n\psi_n + \omega^2\beta_{n+1}\psi_{n+1})\right] = 0. \tag{A.1}$$

In order to eliminate Λ, plug in the value of $\Lambda\psi_m$ and $\Lambda\psi_{m+1}$ given by the rhs of equation (10):

$$\sum_{j\leftrightarrow k} A_{\dots jk\dots}\left[\left(\frac{z_j z_k}{z_{1:N}a}+\frac{z_{1:N}a}{z_j z_k}+z_{1:N}\omega^4 a+\frac{1}{z_{1:N}\omega^4 a}\right)(\omega^{-2}\psi_m+\omega^2\psi_{m+1})z_j\right.$$
$$-z_j\left(z_j^{-1}\omega^{-4}+z_j\right)\sum_{n=m}^{m+N-1}(\omega^{-2}\alpha_n\psi_n+\omega^2\beta_{n+1}\psi_{n+1})\frac{z_{m+1:n}}{z_{n+1:N+m-1}}$$
$$-z_j\left(z_k^{-1}+z_k\omega^4\right)\sum_{n=m+1}^{m+N}(\omega^{-2}\alpha_n\psi_n+\omega^2\beta_{n+1}\psi_{n+1})\frac{z_{m+2:n}}{z_{n+1:N+m}}+(\eta^{-2}+\eta^2 z_j z_k)$$
$$\left.\times\left(\eta^{-2}z_k+\frac{\eta^2}{z_j}\right)\sum_{n=m+1}^{m+N-1}(\omega^{-2}\alpha_n\psi_n+\omega^2\beta_{n+1}\psi_{n+1})\frac{z_{m+2:n}}{z_{n+1:m+N-1}}\right]=0. \qquad \text{(A.2)}$$

We look for a sufficient condition on the scattering amplitude $A_{\dots jk\dots}$ which ensures the validity of the equality (A.2). We start by considering the terms, in the sums, that involve ψ_j for $j\neq m, m+1$ and require their single contribution to be zero. Working out we get the following condition:

$$\sum_{j\leftrightarrow k} A_{\dots jk\dots}\left[\frac{1}{z_j}-\frac{1}{z_k}+z_j z_k^2-z_j^2 z_k+\left(\eta^4+\frac{1}{\eta^4}-\omega^4-\frac{1}{\omega^4}\right)z_k\right]=0. \qquad \text{(A.3)}$$

When $\eta=\omega$ the expression in parenthesis is antisymmetric and the sum vanishes if the scattering amplitude is symmetric $A_{\dots jk\dots}=A_{\dots kj\dots}$. Sorting out the terms ψ_m and ψ_{m+1} in (A.2) we got a more complicate expression which also goes to zero on the previous conditions, but not for the more general solution of (A.3).

References

[1] Jacobsen J L and Kondev J 1998 Field theory of compact polymers on the square lattice *Nucl. Phys.* B **532** 635 (*Preprint* cond-mat/9804048)

[2] Jacobsen J L and Vannimenus J 1999 Finite average lengths in critical loop models *J. Phys. A: Math. Gen.* **32** 5455 (*Preprint* cond-mat/9903242)

[3] Jacobsen J L and Kondev J 2002 Conformal field theory of the Flory model of polymer melting *Preprint* cond-mat/0209247

[4] Jacobsen J L and Kondev J 1999 Transition from the compact to the dense phase of two-dimensional polymers *J. Stat. Phys.* **96** 21 (*Preprint* cond-mat/9811085)

[5] Jacobsen J L 1999 On the universality of fully packed loop models *J. Phys. A: Math. Gen.* **32** 5445 (*Preprint* cond-mat/9903132)

[6] Kondev J and Henley C L 1995 Four-colouring model on the square lattice: a critical ground state *Phys. Rev.* B **52** 6628

[7] Kondev J and Henley C L 1996 Kac–Moody symmetries of critical ground states *Nucl. Phys.* B **464** 540 (*Preprint* cond-mat/9511102)

[8] Kondev J, de Gier J and Nienhuis B 1996 Operator spectrum and exact exponents of the fully packed loop model *J. Phys. A: Math. Gen.* **29** 6489 (*Preprint* cond-mat/9603170)

[9] Kondev J and Jacobsen J L 1998 Conformational entropy of compact polymers *Phys. Rev. Lett.* **81** 2922

[10] Kondev J 1997 Liouville field theory of fluctuating loops *Phys. Rev. Lett.* **78** 4320 (*Preprint* cond-mat/9703113)

[11] Nienhuis B 1982 Exact critical point and critical exponents of O(n) models in two dimensions *Phys. Rev. Lett.* **49** 1062

[12] Nienhuis B 2001 Tiles and colors *J. Stat. Phys.* **102** 981 (*Preprint* cond-mat/0005274)

[13] Lieb E H 1967 Residual entropy of square ice *Phys. Rev.* **162** 162

[14] Baxter R J 1970 Colourings of a hexagonal lattice *J. Math. Phys.* **11** 784

[15] Kostov I K 2002 Exact solution of the three-color problem on a random lattice *Phys. Lett.* B **549** 245 (*Preprint* hep-th/0005190)

[16] Baxter R J 1986 q colourings of the triangular lattice *J. Phys. A: Math. Gen.* **19** 2821
[17] Baxter R J 1987 Chromatic polynomials of large triangular lattices *J. Phys. A: Math. Gen.* **20** 5241
[18] Baxter R J, Kelland S B and Wu F Y 1976 Equivalence of the Potts model or Whitney polynomial with an ice-type model *J. Phys. A: Math. Gen.* **9** 397
[19] Batchelor M T and Blöte H W J 1988 Conformal anomaly and scaling dimensions of the O(n) model from an exact solution on the honeycomb lattice *Phys. Rev. Lett.* **61** 138
[20] Batchelor M T and Blöte H W J 1989 Conformal invariance and critical behavior of the O(n) model on the honeycomb lattice *Phys. Rev.* B **39** 2391
[21] Batchelor M T, Suzuki J and Yung C M 1994 Exact results for hamiltonian walks from the solution of the fully packed loop model on the honeycomb lattice *Phys. Rev. Lett.* **73** 2646 (*Preprint* cond-mat/9408083)
[22] Batchelor M T, Nienhuis B and Warnaar S O 1989 Bethe-ansatz results for a solvable O(n) model on the square lattice *Phys. Rev. Lett.* **62** 2425
[23] Batchelor M T, Blöte H W J, Nienhuis B and Yung C M 1996 Critical behaviour of the fully packed loop model on the square lattice *J. Phys. A: Math. Gen.* **29** L399
[24] Blöte H W J and Nienhuis B 1994 Fully packed loop model on the honeycomb lattice *Phys. Rev. Lett.* **72** 1372
[25] Blöte H W J and Nienhuis B 1989 Critical behaviour and conformal anomaly of the O(n) model on the square lattice *J. Phys. A: Math. Gen.* **22** 1415
[26] Blöte H W J, Nightingale M P and Derrida B 1981 Critical exponents of two-dimensional Potts and bond percolation models *J. Phys. A: Math. Gen.* **14** L45
[27] Reshetikhin N Yu 1991 A new exactly solvable case of an O(n)-model on a hexagonal lattice *J. Phys. A: Math. Gen.* **24** 2387
[28] Kulish P P and Reshetikhin N Yu 1981 Generalized Heisenberg ferromagnet and Gross–Neveu model *Sov. Phys.–JETP* **53** 108
[29] Martins M J 1999 Integrable mixed vertex models from braid monoid algebra *Statistical Physics on the Eve of the 21-st century (vol 14 of Series on Advances in Statistical Mechanics)* ed M T Batchelor and L T Wille (Singapore: World Scientific) (*Preprint* solv-int/9903006)
[30] Domany E, Mukamel D, Nienhuis B and Schwimmer A 1981 Duality relations and equivalence for models with O(n) and cubic symmetry *Nucl. Phys.* B **190** 279
[31] Dotsenko V S, Jacobsen J L and Picco M 2001 Classification of conformal field theories based on coulomb gases. Application to loop models *Nucl. Phys.* B **618** 523 (*Preprint* hep-th/0105287)
[32] Raghavan R, Henley C L and Arouh S L 1997 New two-color dimers models with critical ground state *J. Stat. Phys.* **86** 517 (*Preprint* cond-mat/9606220)
[33] Di Francesco P, Guitter E and Jacobsen J L 2000 Exact meander asymptotics: a numerical check *Nucl. Phys.* B **580** 757 (*Preprint* cond-mat/0003008)
[34] Higuchi S 1999 Compact polymers on decorated square lattices *J. Phys. A: Math. Gen.* **32** 3697 (*Preprint* cond-mat/9811426)
[35] Higuchi S 2000 Loop model with generalized fugacity in three dimensions *J. Phys. A: Math. Gen.* **33** 1661 (*Preprint* cond-mat/9907335)
[36] Glasser M L, Abraham D B and Lieb E H 1972 Analytic properties of the free energy for the Ice models *J. Math. Phys.* **13** 887
[37] Deguchi T 2003 Introduction to solvable lattice models in statistical and mathematical physics *Preprint* cond-mat/0304309
[38] Schultz C L 1981 Solvable q-state models in lattice statistics and quantum field theory *Phys. Rev. Lett.* **46** 629
[39] Stroganov Yu G 1979 A new calculation method for partition functions in some lattice models *Phys. Lett.* A **74** 116